

A kinetic theory derivation of the transport coefficients of stochastic rotation dynamics

C. M. Pooley and J. M. Yeomans

The Rudolph Peierls Centre for Theoretical Physics, 1 Keble Road, Oxford, OX1 3NP, England.

(Dated: September 13, 2004)

We use a kinetic theory approach to derive the continuum Navier-Stokes and heat conduction equations for stochastic rotation dynamics, a particle based algorithm for simulating a fluid. Hence we obtain expressions for the viscosity and thermal conductivity in two and three dimensions. The predictions are tested numerically and good agreement is found.

I. INTRODUCTION

New approaches to modelling hydrodynamics, ranging from cellular automata to lattice Boltzmann, have proved powerful tools to investigate the flow of complex fluids. A particularly simple and appealing algorithm, introduced by Malevanets and Kapral, is stochastic rotation dynamics [1]. This is a particulate approach to solving the equations of motion of a fluid. Particles move in continuous space and discrete time. Collisions between them are treated in a coarse-grained manner but are defined to conserve mass, momentum and energy such that the thermo-hydrodynamic equations of motion are obeyed on sufficiently long length and time scales.

The approach does not seek to accurately simulate a system of interacting particles as is the case in, for example, molecular dynamics. Although this means that molecular details of the system are lost it allows much longer time scales to be accessed. This has allowed new insights into many phenomena in the field of complex fluids. The approach has been used to study the behaviour of polymers [2, 3], colloids [3, 4], flow around objects [5–7] and amphiphilic systems [8, 9].

For example polymers are modelled using a molecular dynamics algorithm for bead-spring chains. The chains are coupled to the fluid through momentum exchange. Locally the polymer beads are buffeted by collisions with the solvent, and so they obey a Langevin-like equation. However when considered in the continuum limit the fluid correctly models the Navier-Stokes equations. Therefore this method captures the microscopic Brownian motion of particles and also the hydrodynamic behaviour of the surrounding fluid.

Because of the simplicity of the algorithm it has been possible to make substantial progress towards understanding its behaviour. Our aim in this paper is to derive the continuum equations of motion modelled by the algorithm using a kinetic theory approach. This allows us to find expressions for the transport coefficients: the viscosity and the thermal conductivity. The remainder of the introduction is devoted to describing the stochastic rotation dynamics algorithm and then summarising previous analytic work on the model.

The variables used in the stochastic rotation dynamics algorithm are a set of particles of masses m_i which move continuously in space with positions $\mathbf{r}_i(t)$ and velocities

$\mathbf{v}_i(t)$. These variables are updated discretely in time t with a time step Δt . The update may be separated into two parts:

(i) A free streaming step in which all the particles are moved according to

$$\mathbf{r}_i(t + \Delta t) = \mathbf{r}_i(t) + \mathbf{v}_i(t)\Delta t. \quad (1)$$

(ii) A collision step. The system is divided up into a grid of square (or cubic) cells of linear dimension l . Within each cell the center of mass velocity,

$$\mathbf{v}_{cm} = \frac{\sum_{i=1}^N m_i \mathbf{v}_i}{\sum_{i=1}^N m_i}, \quad (2)$$

is calculated, where the sum is over the N particles sharing the same cell. The velocities of particles are updated according to

$$\mathbf{v}_i(t + \Delta t) = \mathbf{R}[\mathbf{v}_i(t) - \mathbf{v}_{cm}(t)] + \mathbf{v}_{cm}(t). \quad (3)$$

By multiplying (3) by m_i and summing over all the particles within a cell it is clear that momentum is conserved.

\mathbf{R} the collision matrix is different for each cell. Its choice is determined by a number of factors. For energy conservation it must be orthogonal i.e. $\mathbf{R}^T = \mathbf{R}^{-1}$. Furthermore \mathbf{R} and its inverse must occur with equal probability. This ensures the system is in a state of detailed balance so that the velocities of particles tend toward a Maxwell Boltzmann distribution. Additionally \mathbf{R} must not have a preferred direction or the isotropy of the continuum equations will not be reproduced correctly.

In this paper we choose \mathbf{R} to be a rotation matrix with a fixed angle α but with a rotation axis which is chosen randomly for each cell. The parameter α allows us to tune the viscosity of the fluid as shown below. This is not a unique choice for \mathbf{R} . For example, Ihle and Kroll [10] use an algorithm in which they randomly choose either the x , y or z direction and perform a two dimensional rotation of fixed angle about this axis. This also satisfies the constraints above and has the advantage of a slight increase in computational efficiency.

It was noted by Ihle and Kroll [11] that if the grid is chosen to lie in the same position at each time step then the method suffers from a lack of Galilean invariance, which is most pronounced at low temperatures. This is because if the particles do not travel far at each time step

they tend to collide repeatedly with the same neighbours sharing the cell. This violates the assumption of molecular chaos and results in an unphysical dependence of the transport coefficients on the velocity of the fluid. To overcome this the position of the grid is randomly shifted at each time step.

Malevanets and Kapral [1] showed that the algorithm possesses an H-theorem, ensuring that an isolated system will relax towards the Maxwell Boltzmann distribution. This has the advantage that the approach does not suffer from the numerical instabilities that can make continuum methods difficult to handle. Malevanets and Kapral [1] calculated the transport coefficients in two and three dimension for the rotation angle $\alpha = 90^\circ$. More recently Kikuchi *et al* [12] calculated the shear viscosity for arbitrary angle. The development in this paper gives a more elegant and complete derivation, based on a kinetic theory approach, which also includes the thermal behaviour of the fluid. The transport coefficients have been calculated independently by Ihle and Kroll using a complementary method [10, 13, 14], a discrete-time projection operator technique used to derive the Green-Kubo [15] relations. The two methods agree in the limit that the fluctuations in particle number within the cells is ignored except for a small discrepancy found in the thermal conductivity.

In section II we derive the continuum equations of motion for the stochastic rotation dynamics model. From these we are able to read off expressions for the transport coefficients. In section III we perform numerical simulations to test the theoretical expressions. A discussion of how quickly the fluid reaches a steady state is used to suggest the optimum choice of model parameters.

II. DERIVING THE CONTINUUM CONSERVATION EQUATIONS

A. Summary and notation

In the stochastic rotation dynamics algorithm mass, momentum and energy are all conserved and therefore we expect the continuity, Navier-Stokes, and heat conduction equations to describe the fluid in the continuum limit. In general a conserved quantity Q obeys an evolution equation of the form

$$\partial_t \rho_Q + \partial_\alpha j_\alpha = 0 \quad (4)$$

where ρ_Q is the density of Q and \mathbf{j} is its flux. In the simulations time is discretized and we must take account of a finite time step Δt . It is convenient to define \mathbf{j} as the flux of Q across a plane between the times t and $t + \Delta t$ based on quantities at time t . In this case the conservation equation (4) becomes

$$\partial_t \rho_Q + \partial_\alpha \left(j_\alpha - \frac{\Delta t}{2} \partial_t j_\alpha \right) = O(\delta^3). \quad (5)$$

The quantity δ denotes the magnitude of any gradient, which is taken to be small.

For simplicity we assume that all the particles have equal mass $m_i = m$. We also assume that the system contains a very large number of particles such that each position \mathbf{r} has a well defined particle distribution function $f(\mathbf{v}, \mathbf{r})$, which gives the mass density of particles traveling with velocity \mathbf{v} . The mass and momentum density are given by

$$\rho(\mathbf{r}) = \int_{-\infty}^{\infty} d\mathbf{v} f, \quad \rho \mathbf{u}(\mathbf{r}) = \int_{-\infty}^{\infty} d\mathbf{v} \mathbf{v} f. \quad (6)$$

The average of a quantity X is defined by

$$\langle X(\mathbf{r}) \rangle = \frac{1}{\rho(\mathbf{r})} \int_{-\infty}^{\infty} d\mathbf{v} X f. \quad (7)$$

We will use the abbreviation $M_{\alpha\beta\dots} = \langle (v_\alpha - u_\alpha)(v_\beta - u_\beta) \dots \rangle$. The temperature is defined using the parameter $\theta = \frac{k_B T}{m} = \frac{1}{d} \sum_\alpha M_{\alpha\alpha}$.

Firstly we outline the procedure we use. We write an expression for the flux \mathbf{j} crossing a square area (or line in two dimensions) during the streaming step. The axes are positioned such that the area (line) is centered at the origin. We assume that the system is in local equilibrium and hence the spatial dependence of f can be written in terms of the thermodynamic variables. This allows us to write the flux in terms of moments of the distribution function at the origin. Steady state values for the moments can be calculated by separately considering the streaming and collision steps. Hence we obtain expressions for the conservation equations (20, 24, 32) from which we can read off the transport coefficients. Furthermore we find that momentum transfer within the collision step provides an additional contribution to the viscosity (71, 73).

B. Calculating the flux

We now perform the detailed calculation. In three dimensions we consider flux in the y direction through the area bounded by the points $(\pm \frac{a}{2}, 0, \pm \frac{a}{2})$, and in two dimensions the flux across the line section connecting the two points $(\pm \frac{a}{2}, 0)$. The flux is given by

$$j_y = \frac{1}{a^{d-1} \Delta t} \int_{-\infty}^{\infty} d\mathbf{v} \int_A d\mathbf{r} \frac{Q}{m} f \quad (8)$$

where d is the dimension of the system. The integral \int_A is over the volume of particles with a particular velocity \mathbf{v} which cross the area during the streaming step and may be expressed as

$$\int_A d\mathbf{r} = \int_{-v_y \Delta t}^0 dr_y \prod_\tau \int_{-\frac{a}{2} + \frac{v_\tau}{v_y} r_y}^{\frac{a}{2} + \frac{v_\tau}{v_y} r_y} dr_\tau, \quad (9)$$

where τ is x in two dimensions, and x and z in three dimensions. In two dimensions this is illustrated by the shaded area in figure 1(a).

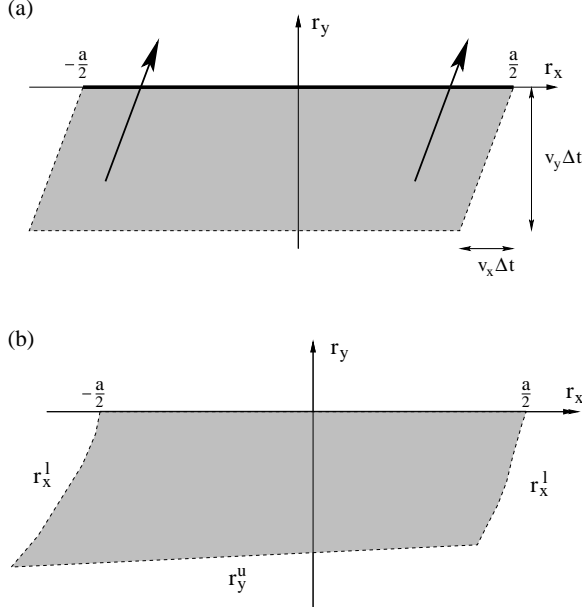


FIG. 1: The shaded region shows the area of fluid from which particles with velocity \mathbf{v} pass through the line $-a/2 \leq x \leq a/2$. (a) The original co-ordinate system. (b) The transformed co-ordinate system (see equation (16)).

The thermodynamic variables may be Taylor expanded about the origin

$$\begin{aligned}\theta &= \theta_0 + (\partial_\alpha \theta) r_\alpha + O(\delta^2), \\ \rho &= \rho_0 + (\partial_\alpha \rho) r_\alpha + O(\delta^2), \\ u_\beta &= u_{0\beta} + (\partial_\alpha u_\beta) r_\alpha + O(\delta^2).\end{aligned}\quad (10)$$

We also assume that \mathbf{u}_0 is $O(\delta)$. This is justified because stochastic rotation dynamics is Galilean invariant and a transformation can be made to make \mathbf{u}_0 arbitrarily small. Now and subsequently we ignore all terms of $O(\delta^2)$. Care must be taken in the calculation because both \mathbf{u}_0 and $\partial_\alpha \mathbf{u}$ are $O(\delta)$, and so the discarding of higher order terms must only be done after all derivatives have been multiplied out.

We approximate the system to be in local thermodynamic equilibrium. Therefore we expect the spatial dependence of f to arise from the thermodynamic variables: the local average mass density ρ , the average velocity \mathbf{u} , and the temperature θ . Because of the Galilean invariance of the method f only depends upon $\mathbf{v} - \mathbf{u}$. Since θ has units of velocity squared then generally we may write

$$f d\mathbf{v} = \frac{\rho}{\theta^{\frac{d}{2}}} g\left(\frac{\mathbf{v} - \mathbf{u}}{\sqrt{\theta}}\right) d\mathbf{v}, \quad (11)$$

where g is a function of a dimensionless variable. In global equilibrium the correspondence with the Maxwell Boltzmann distribution is clear, as in this case g is

$e^{-\frac{(\mathbf{v}-\mathbf{u})^2}{2\theta}}$. Near to global equilibrium g is slightly distorted reflecting any density, velocity or temperature gradients in the system. The only non-zero moments to fourth order for the Maxwell Boltzmann distribution are $M_{xx} = M_{yy} = M_{zz} = \theta$, $M_{xxyy} = M_{yyzz} = M_{zzxx} = \theta^2$ and $M_{xxxx} = M_{yyyy} = M_{zzzz} = 3\theta^2$. The distortion contributes a term of $O(\delta)$ to each moment.

In equation (11) we make the change of variables

$$\frac{\mathbf{v}' - \mathbf{u}_0}{\sqrt{\theta_0}} = \frac{\mathbf{v} - \mathbf{u}}{\sqrt{\theta}} \quad (12)$$

or, written in terms of \mathbf{v} using equation (10),

$$v_\beta = v'_\beta \left[1 + \left(\frac{\partial_\alpha \theta}{2\theta_0} + \frac{\partial_\alpha u_\beta}{v'_\beta} \right) r_\alpha \right]. \quad (13)$$

This allows us to write the flux (8) as

$$j_y = \frac{1}{a^{d-1} \Delta t} \int_{-\infty}^{\infty} d\mathbf{v}' \int_{A'} d\mathbf{r} \frac{Q}{m} \left[1 + \left(\frac{\partial_\alpha \rho}{\rho_0} \right) r_\alpha \right] f \quad (14)$$

where $f(\mathbf{v}', \mathbf{0})$ is now the distribution of particles at the origin. After the change of variables the integration area A' is slightly different. Figure 1(b) illustrates this in two dimensions. From (13)

$$\frac{v_\tau}{v_y} = \frac{v'_\tau}{v'_y} \left[1 + \left(\frac{\partial_\alpha u_\tau}{v'_\tau} - \frac{\partial_\alpha u_y}{v'_y} \right) r_\alpha \right] \quad (15)$$

and we find to first order the upper and lower limits on the x integral and the lower limit of the y integral in equation (9) in two dimensions are given by

$$\begin{aligned}r_x^u &= \frac{a}{2} + \frac{v'_x}{v'_y} \left[1 + \left(\frac{\partial_x u_x}{v'_x} - \frac{\partial_x u_y}{v'_y} \right) \left(\frac{a}{2} + \frac{v'_x}{v'_y} r_y \right) \right. \\ &\quad \left. + \left(\frac{\partial_y u_x}{v'_x} - \frac{\partial_y u_y}{v'_y} \right) r_y \right] r_y, \\ r_x^l &= -\frac{a}{2} + \frac{v'_x}{v'_y} \left[1 + \left(\frac{\partial_x u_x}{v'_x} - \frac{\partial_x u_y}{v'_y} \right) \left(-\frac{a}{2} + \frac{v'_x}{v'_y} r_y \right) \right. \\ &\quad \left. + \left(\frac{\partial_y u_x}{v'_x} - \frac{\partial_y u_y}{v'_y} \right) r_y \right] r_y, \\ r_y^l &= -\Delta t v'_y \left[1 + \left(\frac{\partial_x \theta}{2\theta_0} + \frac{\partial_x u_y}{v'_y} \right) r_x \right. \\ &\quad \left. - \left(\frac{\partial_y \theta}{2\theta_0} + \frac{\partial_y u_y}{v'_y} \right) \Delta t v'_y \right].\end{aligned}\quad (16)$$

Similar but longer expressions apply in three dimensions. To first order the area bounded by these curves is

$$\begin{aligned}A &= a^{d-1} \Delta t v'_y - a^{d-1} \Delta t^2 \left[\frac{1}{2} \sum_\tau (v'_y \partial_\tau u_\tau - v'_\tau \partial_\tau u_y) \right. \\ &\quad \left. + \left(\frac{v_y'^2 \partial_y \theta}{2\theta_0} + v'_y \partial_y u_y + \sum_\tau \left(\frac{v'_\tau v'_y \partial_\tau \theta}{2\theta_0} + v'_\tau \partial_\tau u_y \right) \right) \right].\end{aligned}\quad (17)$$

The second and third terms come from a shift in the sides and the lower edge respectively.

For the terms of $O(\delta)$ in (14) it is sufficient to approximate $\mathbf{v} = \mathbf{v}'$, and using equation (9), we find

$$\int_A d\mathbf{r} \ r_\alpha = -\frac{a^{d-1} \Delta t^2}{2} v'_y v'_\alpha. \quad (18)$$

C. Mass transport

To calculate the mass flux we set $Q = m$ in equation (14), and find that $j_y = \rho u_y - \frac{\Delta t}{2} \partial_y(\rho\theta)$. The 0 subscript is now omitted since this is true for all points. Because of the symmetry $j_\alpha = \rho u_\alpha - \frac{\Delta t}{2} \partial_\alpha(\rho\theta)$, and equation (5) becomes

$$\partial_t \rho + \partial_\alpha \left(\rho u_\alpha - \frac{\Delta t}{2} [\partial_t(\rho u_\alpha) + \partial_\alpha(\rho\theta)] \right) = 0. \quad (19)$$

We later find (see equation (24)) that $\partial_t(\rho u_\alpha) + \partial_\alpha(\rho\theta) = O(\delta^2)$ is the first order approximation to the Navier-Stokes equation. Therefore (19) becomes, to second order, the familiar continuity equation

$$\partial_t \rho + \partial_\alpha(\rho u_\alpha) = 0. \quad (20)$$

D. Momentum transport

Next we consider $Q = mv_x$. We denote the flux of x momentum across a plane of constant y by T_{xy} . Substituting (13) into (14), and using the results (17) and (18) gives

$$T_{xy} = \rho \left[u_x u_y + M_{xy} - \frac{\theta \Delta t}{2} (\partial_x u_y + \partial_y u_x) \right]. \quad (21)$$

By setting $Q = mv_y$ we may use (14) to find T_{yy} . Since we can cyclically permute the labels x , y and z , we can construct the complete momentum flux tensor

$$T_{\alpha\beta} = \rho u_\alpha u_\beta + \rho M_{\alpha\beta} - \frac{\rho\theta\Delta t}{2} \times (\partial_\alpha u_\beta + \partial_\beta u_\alpha + \delta_{\alpha\beta} \nabla \cdot \mathbf{u}). \quad (22)$$

The pressure term which appears in the Navier-Stokes equations can be removed from the second term in (22). For instance in two dimension $\rho M_{xx} = p + \rho \frac{1}{2} (M_{xx} - M_{yy})$ where $p = \rho\theta$ is the ideal gas pressure. We use

$$\partial_t T_{\alpha\beta} = \delta_{\alpha\beta} \partial_t(\rho\theta) = -\left(\frac{2}{d} + 1\right) \delta_{\alpha\beta} \rho\theta \nabla \cdot \mathbf{u} \quad (23)$$

which is the first order approximation to the heat conduction equation derived below (see equation (32)). The conservation equation (5) then becomes the Navier-Stokes equation

$$\partial_t(\rho u_\alpha) + \partial_\beta(\rho u_\alpha u_\beta) = -\partial_\alpha p + \partial_\beta \sigma_{\alpha\beta}, \quad (24)$$

where

$$\sigma_{\alpha\beta} = \frac{\rho\theta\Delta t}{2} \left(\partial_\alpha u_\beta + \partial_\beta u_\alpha - \frac{2}{d} \delta_{\alpha\beta} \nabla \cdot \mathbf{u} \right) - \rho M'_{\alpha\beta}, \quad (25)$$

with $M'_{\alpha\beta} = M_{\alpha\beta}$ for $\alpha \neq \beta$. In two dimensions

$$M'_{xx} = -M'_{yy} = \frac{1}{2} (M_{xx} - M_{yy}), \quad (26)$$

and in three dimensions

$$\begin{aligned} M'_{xx} &= \frac{1}{3} (M_{xx} - M_{yy}) + \frac{1}{3} (M_{xx} - M_{zz}), \\ M'_{yy} &= \frac{1}{3} (M_{yy} - M_{xx}) + \frac{1}{3} (M_{yy} - M_{zz}), \\ M'_{zz} &= \frac{1}{3} (M_{zz} - M_{xx}) + \frac{1}{3} (M_{zz} - M_{yy}). \end{aligned} \quad (27)$$

E. Energy transport

Finally, we derive the energy transport equation by setting $Q = \frac{1}{2} m v^2 = \frac{1}{2} m \sum_\beta v_\beta^2$. Using (14) we find

$$\begin{aligned} q_\alpha &= \left(\frac{d+2}{2} \right) \rho \theta u_\alpha + \frac{\rho}{2} \sum_\beta M_{\beta\beta\alpha} \\ &\quad - \left(\frac{d+2}{4} \right) \theta \Delta t (\theta \partial_\alpha \rho + 2\rho \partial_\alpha \theta) \end{aligned} \quad (28)$$

and the conservation equation (5)

$$\partial_t \left(\frac{\rho}{2} \langle v^2 \rangle \right) + \partial_\alpha \left(q_\alpha - \frac{\Delta t}{2} \partial_t q_\alpha \right) = 0. \quad (29)$$

The energy density in a system can be divided into two contributions, $\frac{1}{2} \rho \langle v^2 \rangle = \frac{d}{2} \rho\theta + \frac{1}{2} \rho u^2$, one from thermal motion and the other from bulk motion of the fluid. The rate of change of energy associated with bulk flow may be rewritten

$$\partial_t \left(\frac{\rho u^2}{2} \right) = u_\alpha \partial_t(\rho u_\alpha) - \frac{u^2 \partial_t \rho}{2}. \quad (30)$$

Using the results derived above, $\partial_t \rho = -\partial_\alpha(\rho u_\alpha) + O(\delta^2)$ from the continuity equation (20) and $\partial_t(\rho u_\alpha) = -\partial_\alpha p + O(\delta^2)$ from the Navier-Stokes equation (24), equation (30) becomes

$$\partial_t \left(\frac{\rho u^2}{2} \right) = -u_\alpha \partial_\alpha p + \frac{u^2 \partial_\alpha(\rho u_\alpha)}{2}. \quad (31)$$

The second term on the right hand side can be neglected as it is $O(\delta^3)$. The balance of the remaining terms simply states that the rate of change of energy in the bulk flow is equal to the work done by the force acting on a fluid element resulting from any pressure gradients present. Substituting this into (29) we finally obtain the heat conduction equation,

$$\partial_t \left(\frac{d}{2} \rho\theta \right) + \partial_\alpha \left(\frac{d}{2} \rho\theta u_\alpha \right) = -\rho\theta \partial_\alpha u_\alpha + \partial_\alpha(\kappa \partial_\alpha \theta) \quad (32)$$

where the thermal conductivity is

$$\kappa = \rho\theta\Delta t \left(\frac{d+2}{4} \right) - \frac{\rho \sum_{\beta} M_{\beta\beta\alpha}}{\partial_{\alpha}\theta}. \quad (33)$$

To calculate the moments M in equations (25) and (33) we must separately consider the effect of the streaming and collision operations.

F. The effect of streaming on the moments

Particles which are at the origin moving with velocity \mathbf{v} after the streaming step come from a region at position $-\mathbf{v}\Delta t$. Therefore

$$f^a(\mathbf{v}, \mathbf{0}) d\mathbf{v} = f^b(\mathbf{v}, -\mathbf{v}\Delta t) d\mathbf{v} \quad (34)$$

where the superscripts b and a denote before and after streaming. We assume the form (11) to convert the right hand side of equation (34) into the distribution function at the origin. We substitute $\mathbf{r} = -\mathbf{v}\Delta t$ into equation (13) and make the change of variables

$$v_{\beta} = v'_{\beta} \left[1 - \Delta t v'_{\alpha} \left(\frac{\partial_{\alpha}\theta}{2\theta_0} + \frac{\partial_{\alpha}u_{\beta}}{v'_{\beta}} \right) \right]. \quad (35)$$

Evaluating the Jacobian this results in

$$d\mathbf{v} = \left[1 - \Delta t \left(\frac{d+1}{2} v'_{\alpha} \frac{\partial_{\alpha}\theta}{\theta_0} + \partial_{\alpha}u_{\alpha} \right) \right] d\mathbf{v}' \quad (36)$$

and we find

$$f^a d\mathbf{v} = \left[1 - \Delta t \left(\frac{v'_{\alpha}\partial_{\alpha}\rho}{\rho_0} + \frac{v'_{\alpha}\partial_{\alpha}\theta}{2\theta_0} + \partial_{\alpha}u_{\alpha} \right) \right] f^b d\mathbf{v}'. \quad (37)$$

Since all variables are evaluated at the origin we subsequently omit the subscript 0.

We use relation (37) to find how the moments M change during streaming. The zeroth and first moments are

$$\rho^a = \rho^b - \rho^b \Delta t \partial_{\alpha}u_{\alpha}, \quad (38)$$

$$\rho^a u_{\alpha}^a = \rho^b u_{\alpha}^b - \Delta t \partial_{\alpha}(\rho\theta). \quad (39)$$

These are the continuity and Navier-Stokes equations to a first approximation. The calculations are simplified somewhat if we choose $u_{\alpha}^b = 0$.

The change in correlations between v_x and v_y can be calculated. For example

$$\begin{aligned} M_{xy}^a &= \frac{1}{\rho^a} \int_{-\infty}^{\infty} d\mathbf{v} (v_x - u_x^a)(v_y - u_y^a) f^a \\ &= M_{xy}^b - \theta\Delta t (\partial_y u_x + \partial_x u_y). \end{aligned} \quad (40)$$

More generally we find that

$$M_{\alpha\beta}^a = M_{\alpha\beta}^b - \theta\Delta t (\partial_{\alpha}u_{\beta} + \partial_{\beta}u_{\alpha}). \quad (41)$$

Changes in the third order moments are given by

$$\begin{aligned} M_{\alpha\alpha\alpha}^a &= M_{\alpha\alpha\alpha}^b - 3\theta\Delta t \partial_{\alpha}\theta, \\ M_{\beta\beta\alpha}^a &= M_{\beta\beta\alpha}^b - \theta\Delta t \partial_{\alpha}\theta, \quad \alpha \neq \beta, \\ M_{\gamma\beta\alpha}^a &= M_{\gamma\beta\alpha}^b, \quad \alpha \neq \beta \neq \gamma. \end{aligned} \quad (42)$$

G. The effect of collisions on the moments

The effect of the collision step is to update the velocities according to equation (3). In two dimensions (3) can be written

$$\mathbf{v}^a = \begin{pmatrix} \cos(\alpha) & \pm \sin(\alpha) \\ \mp \sin(\alpha) & \cos(\alpha) \end{pmatrix} (\mathbf{v}^b - \mathbf{v}_{\mathbf{cm}}) + \mathbf{v}_{\mathbf{cm}} \quad (43)$$

where b and a denote before and after the collision. There is no superscript on $\mathbf{v}_{\mathbf{cm}}$ since this is unchanged by the collision. The sign in the matrix is chosen randomly according to whether the rotation axis is up or down.

$\mathbf{v}_{\mathbf{cm}}$ can be written as $\frac{1}{N}\mathbf{v} + \frac{N-1}{N}\mathbf{v}^s$ where $\mathbf{v}^s = \frac{1}{N-1} \sum_{i=1}^{N-1} v_i$. The first term refers to the particle whose velocity is being updated and the second to the other $(N-1)$ particles sharing the same cell. We assume that the velocities of different particles within the same cell are uncorrelated: this is the approximation of molecular chaos. Therefore we may write $\langle (v_x - u_x)(v_y^s - u_y) \rangle = \langle (v_x^s - u_x)(v_y - u_y) \rangle = 0$ and $\langle (v_x^s - u_x)(v_y^s - u_y) \rangle = \frac{1}{N-1} \langle (v_x - u_x)(v_y - u_y) \rangle$, where the average is taken over the velocity distribution functions of the particles.

Using these formulae to simplify the expression for M_{xy} which follows from equation (43), and averaging over the two directions of the rotation axis ($\pm\alpha$), gives

$$M_{xy}^a = \left[1 - \left(\frac{N-1}{N} \right) (1 - \cos(2\alpha)) \right] M_{xy}^b. \quad (44)$$

In the simulations the number of particles N in a given cell is not constant. These fluctuations can be important as the simulations are often run with $N \sim 5$. The probability of N particles being in a box is given by the Poisson distribution $P_d = \frac{e^{-\gamma} \gamma^N}{N!}$. γ is the average particle number per cell which is related to the mass density by $\gamma = \frac{\rho^d}{m}$. The probability of a given particle being in a box which contains a total of N particles is $\frac{NP_d}{\gamma}$. Taking this into account gives

$$M_{xy}^a = w M_{xy}^b \quad (45)$$

where

$$w = \left[1 - \left(\frac{\gamma - 1 + e^{-\gamma}}{\gamma} \right) [1 - \cos(2\alpha)] \right]. \quad (46)$$

Similarly we find that

$$\begin{pmatrix} M_{xx} \\ M_{yy} \end{pmatrix}^a = \begin{pmatrix} G_{11} & G_{12} \\ G_{21} & G_{22} \end{pmatrix} \begin{pmatrix} M_{xx} \\ M_{yy} \end{pmatrix}^b \quad (47)$$

where

$$\begin{aligned} G_{11} = G_{22} &= \frac{1}{\gamma} [1 - e^{-\gamma} + (\gamma - 1 + e^{-\gamma}) \cos^2(\alpha)], \\ G_{12} = G_{21} &= \frac{1}{\gamma} [\gamma - 1 + e^{-\gamma}] \sin^2(\alpha). \end{aligned} \quad (48)$$

This results in

$$M_{xx}^a - M_{yy}^a = w (M_{xx}^b - M_{yy}^b). \quad (49)$$

A similar calculation gives

$$\begin{pmatrix} M_{yyyy} \\ M_{xxy} \end{pmatrix}^a = \begin{pmatrix} K_{11} & K_{12} \\ K_{21} & K_{22} \end{pmatrix} \begin{pmatrix} M_{yyyy} \\ M_{xxy} \end{pmatrix}^b, \\ \begin{pmatrix} M_{xxx} \\ M_{yyx} \end{pmatrix}^a = \begin{pmatrix} K_{11} & K_{12} \\ K_{21} & K_{22} \end{pmatrix} \begin{pmatrix} M_{xxx} \\ M_{yyx} \end{pmatrix}^b, \quad (50)$$

where

$$\begin{aligned} K_{11} &= \frac{1}{N^2} [1 + 3(N-1) \cos^2(\alpha) \\ &\quad + (2-3N+N^2) \cos^3(\alpha)], \\ K_{12} &= \frac{3}{N^2} [N-1] [1 + (2-N) \cos(\alpha)] \sin^2(\alpha), \\ K_{21} &= \frac{1}{N^2} [N-1] [1 + (2-N) \cos(\alpha)] \sin^2(\alpha), \\ K_{22} &= \frac{1}{4N^2} [2 + 2N + (2-3N+N^2) [\cos(\alpha) + 3 \cos(3\alpha)] \\ &\quad + 10(N-1) \cos(2\alpha)]. \end{aligned} \quad (51)$$

To take into account particle number fluctuations equations (51) should be averaged over a Poisson distribution for N . Unfortunately this does not give a simple analytic solution due to the presence of the $\frac{1}{N^2}$ terms. However we note that in going from (44) to (46) the only consequence of particle number variation is the introduction of a term $e^{-\gamma}$. This is negligible for densities $\gamma > 5$, therefore we simply replace N by γ in (51). This is justified in Section III B where we find good agreement between simulation results and theoretical predictions.

In three dimensions the calculation is more involved due to the increased complexity of the rotation matrix. We find

$$\begin{aligned} M_{\alpha\beta}^a &= w M_{\alpha\beta}^b, \quad \alpha \neq \beta, \\ M_{\alpha\alpha}^a - M_{\beta\beta}^a &= w (M_{\alpha\alpha}^b - M_{\beta\beta}^b) \end{aligned} \quad (52)$$

where

$$w = \left[1 - \left(\frac{\gamma-1+e^{-\gamma}}{5\gamma} \right) [4 - 2 \cos(\alpha) - 2 \cos(2\alpha)] \right]. \quad (53)$$

$$\begin{pmatrix} M_{\beta\beta\alpha} \\ M_{\alpha\alpha\alpha} \\ M_{\tau\tau\alpha} \end{pmatrix}^a = \begin{pmatrix} K_{11} & K_{12} & K_{13} \\ K_{21} & K_{22} & K_{23} \\ K_{31} & K_{32} & K_{33} \end{pmatrix} \begin{pmatrix} M_{\beta\beta\alpha} \\ M_{\alpha\alpha\alpha} \\ M_{\tau\tau\alpha} \end{pmatrix}^b \quad (54)$$

where $\alpha \neq \beta \neq \tau$, and

$$\begin{aligned} K_{11} = K_{33} &= \frac{1}{105\gamma^2} [19\gamma^2 + 34\gamma + 52 + (38\gamma^2 - 2\gamma - 36) \cos(\alpha) \\ &\quad + 8(3\gamma^2 + 5\gamma - 8) \cos(2\alpha) + 24(\gamma^2 - 3\gamma + 2) \cos(3\alpha)], \\ K_{22} &= \frac{3}{105\gamma^2} [9\gamma^2 + 22\gamma + 4 + 2(9\gamma^2 - 13\gamma + 4) \cos(\alpha) \end{aligned}$$

$$\begin{aligned} &+ 4(\gamma^2 + 4\gamma - 5) \cos(2\alpha) + 4(\gamma^2 - 3\gamma + 2) \cos(3\alpha)], \\ K_{12} = K_{13} &= \frac{1}{3} K_{21} = \frac{1}{3} K_{23} = K_{31} = K_{32} = \frac{4(\gamma-1)}{105\gamma^2} \times \\ &[11\gamma - 1 + 2(9\gamma - 11) \cos(\alpha) + 6(\gamma-2) \cos(2\alpha)] \sin^2\left(\frac{\alpha}{2}\right). \end{aligned} \quad (55)$$

H. Calculating the moments in the steady state

We now use the results from sections II F and II G to find steady state solutions for the unknown moments in equations (25) and (33). Firstly we consider M_{xy} . Equation (40) states that streaming reduces M_{xy} by an amount $(\partial_y u_x + \partial_x u_y) \theta \Delta t$ and equations (45) and (52) show that the collision step changes the moment by a multiplicative factor w . If the system is in a steady state then applying both these operation consecutively leaves the moments unchanged. Therefore

$$[M_{xy} - (\partial_y u_x + \partial_x u_y) \theta \Delta t] w = M_{xy}. \quad (56)$$

Rearranging and giving the slightly more general result

$$M_{\alpha\beta} = -\theta (\partial_\beta u_\alpha + \partial_\alpha u_\beta) \Delta t \left(\frac{w}{1-w} \right) \quad (57)$$

for $\alpha \neq \beta$.

A similar argument, using (41), (49) and (52) gives

$$M_{\alpha\alpha} - M_{\beta\beta} = -2\theta (\partial_\alpha u_\alpha - \partial_\beta u_\beta) \Delta t \left(\frac{w}{1-w} \right). \quad (58)$$

Substituting (57) and (58) into (25) gives the final result [16]

$$\sigma_{\alpha\beta} = \eta^{kin} \left(\partial_\alpha u_\beta + \partial_\beta u_\alpha - \frac{2}{d} \delta_{\alpha\beta} \nabla \cdot \mathbf{u} \right) \quad (59)$$

where

$$\eta^{kin} = \rho \theta \Delta t \left(\frac{1}{1-w} - \frac{1}{2} \right) \quad (60)$$

with w for two and three dimensions given in equations (46) and (53) respectively. This kinetic contribution to the stress tensor is the same as that for an ideal gas.

To calculate the steady state thermal conductivity values for the third moments of M are required. Using equations (42), (50), and (54) gives

$$\sum_\beta M_{\beta\beta\alpha} = -\frac{a}{b} \partial_\alpha \theta \quad (61)$$

where in two dimensions

$$\begin{aligned} a &= 2\theta \Delta t [2\gamma - 1 + (2 - 3\gamma + \gamma^2) \cos(\alpha) \\ &\quad + (\gamma - 1) \cos(2\alpha)] \\ b &= (\gamma - 1) [\gamma + 2 \cos(\alpha)] \sin^2\left(\frac{\alpha}{2}\right), \end{aligned} \quad (62)$$

and in three dimensions

$$\begin{aligned} a &= 5\theta\Delta t [-4 + 14\gamma + 5\gamma^2 + 2(6 - 11\gamma + 5\gamma^2)\cos(\alpha) \\ &\quad + 8(\gamma - 1)\cos(2\alpha)], \\ b &= 8(\gamma - 1)[2 + 5\gamma + 8\cos(\alpha)]\sin^2\left(\frac{\alpha}{2}\right). \end{aligned} \quad (63)$$

Substituting equation (61) into (33) gives the thermal conductivity

$$\kappa = \rho\theta\Delta t \left(\frac{d+2}{4} + \frac{a}{b} \right). \quad (64)$$

Finally we consider when steady state conditions are applicable. The time evolution of the moment M_{xy} can be written

$$M_{xy}(t + \Delta t) - M_{xy}^{ss} = w [M_{xy}(t) - M_{xy}^{ss}] \quad (65)$$

where M_{xy}^{ss} is the steady state value (57). Provided $|w| < 1$, which it always is, the moment converges towards the steady state value on a time scale given by $\frac{\Delta t}{1-|w|}$. Provided all other time scales in the simulation are significantly longer, then this will be the fastest relaxation process, and the steady state condition will be satisfied. However if there are very fast processes, for example very high frequency shear oscillations, then the effective value of the viscosity will change.

I. Calculation of the collisional viscosity

We have just calculated the kinetic contribution to the stress tensor. This results from movement of the particles and is analogous to the term one would expect for an ideal gas. There is a second contribution to the viscosity because, during the collision step, momentum is moved between the particles within a given cell. We shall denote this term η_{col} . It is analogous to the collisional viscosity which dominates in a fluid which arises from momentum transfer due to intermolecular forces.

To calculate η_{col} we consider an initial velocity distribution

$$\mathbf{u} = \mathbf{u}_0 + (\partial_\alpha \mathbf{u})r_\alpha + O(\delta^2) \quad (66)$$

where \mathbf{r} is now the distance from the center of a cell.

We first consider two dimensions and use the collision equation (43) to relate the x -component of the velocity before and after the collision. Averaging over the two directions of the rotation axis ($\pm\alpha$) and the velocities of the $(N-1)$ particles sharing the same cell gives

$$(v_x^a - u_{x0}) = \left[\frac{1}{N} + \cos(\alpha) \left(1 - \frac{1}{N} \right) \right] (v_x^b - u_{x0}). \quad (67)$$

Next we average over all possible velocities v_x and also take into account particle number fluctuations by averaging, as before, over the probability of any given particle

being in a box which contains N particles $\frac{NP_d}{\gamma}$. Using (66) this gives

$$u_x^a - u_{0x} = g(u_x^b - u_{0x}) = g(\partial_\alpha u_x)r_\alpha \quad (68)$$

where

$$g = \left[1 - \left(\frac{\gamma - 1 + e^{-\gamma}}{\gamma} \right) [1 - \cos(\alpha)] \right]. \quad (69)$$

Consider a plane at constant $y = c$, where c is in the interval $[-\frac{l}{2}, \frac{l}{2}]$. The x momentum crossing it during the collision step can be found by calculating how the total momentum within the cell above the plane changes:

$$\begin{aligned} T_{xy}^{col} &= \frac{\rho}{l\Delta t} \int_{-\frac{l}{2}}^{\frac{l}{2}} dr_x \int_c^{\frac{l}{2}} dr_y (g-1)(r_x \partial_x u_x + r_y \partial_y u_x) \\ &= -\frac{\rho}{\Delta t} (1-g) \left(\frac{l^2}{8} - \frac{c^2}{2} \right) \partial_y u_x. \end{aligned} \quad (70)$$

The position of the grid at each time step is random and hence c takes values between $-\frac{l}{2}$ and $\frac{l}{2}$ with equal probability. Averaging over c we find that $T_{xy}^{col} = -\eta_{col}^{2D} \partial_y u_x$ where

$$\eta_{col}^{2D} = (\gamma - 1 + e^{-\gamma}) \frac{m [1 - \cos(\alpha)]}{12\Delta t}. \quad (71)$$

We can use a similar argument to find the other terms in the moment flux tensor. We find that the collisional stress tensor is given by

$$\sigma_{\alpha\beta}^{col} = -T_{\alpha\beta}^{col} = \eta_{col} \partial_\beta u_\alpha. \quad (72)$$

In three dimensions a similar expression holds with

$$\eta_{col}^{3D} = (\gamma - 1 + e^{-\gamma}) \frac{m [1 - \cos(\alpha)]}{18l\Delta t}. \quad (73)$$

Note that the collisional viscosity depends on the parameters of the model in a different way to the kinetic contribution. The above argument measures momentum flux passing through a plane parallel to the grid. It is not hard to show that $\sigma_{\alpha\beta}^{col}$ is rotationally invariant, hence independent of the orientation of the grid.

III. NUMERICAL TESTS OF THE CONTINUUM EQUATIONS

A. Shear viscosity

To test the off-diagonal elements of the stress tensor (59) we consider a system under shear. The shear is produced using Lees-Edwards boundary conditions [17, 18], as described for stochastic rotation dynamics by Kikuchi *et al.* [12]. These mimic the effect of an infinite system and are a generalization of periodic boundary condition for systems under shear.

We consider the shear to be in the x direction giving a steady state velocity profile $u_x = \dot{\gamma}y$. Thus the only non-zero velocity gradient is $\partial_y u_x = \dot{\gamma}$. Periodic boundary condition are applied in the x and z directions. Particles that leave $y = 0$ appear at $y = L_y$ as for a periodic boundary. However the x velocity is updated by $v_x^{new} = v_x^{old} + v^{shear}$ and the x position is shifted by $x^{new} = x^{old} + v^{shear}t$. Correspondingly particles leaving $y = L_y$ enter at $y = 0$ with $v_x^{new} = v_x^{old} - v$ and $x^{new} = x^{old} - v^{shear}t$.

The energy of sheared systems increased because of viscous heating. Therefore to obtain a steady state it is necessary to introduce a thermostat. This is done by firstly subtracting the shear velocity profile from the particles. The velocities are then rescaled such that the average energy per particle agrees with equipartition of energy $\langle \mathbf{v}^2 \rangle = \theta d$. The shear profile is then added back.

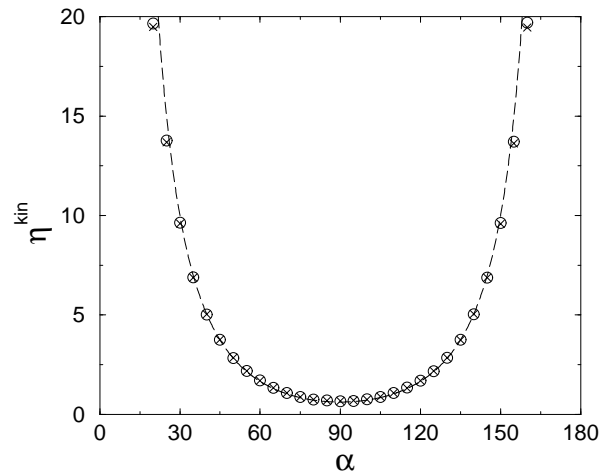
To measure the kinetic viscosity we consider a plane in the system and measure the momentum flux crossing it. Figure 2 show the results of simulations. The system size in two dimensions was $L_x = 50$, $L_y = 50$ and the average was taken over 50000 iterations. In three dimensions $L_x = 50$, $L_y = 50$ and $L_z = 10$ and the average was taken over 5000 iterations. The shear rate was $\dot{\gamma} = 0.02$ and the average particle number per cell was $\gamma = 5$ in both cases. We define $\eta_{xy}^{kin} = \sigma_{xy}^{kin} / \dot{\gamma}$. This was measured by considering a plane at constant y whereas $\eta_{yx}^{kin} = \sigma_{yx}^{kin} / \dot{\gamma}$ was found from a plane at constant x .

We find very good agreement between the theory and simulation results. Deviations occur at small rotation angles. This is a finite size effect. The effective mean free path of particles becomes larger than the size of the system, so the assumption of being near equilibrium is violated. In the extreme case of rotation angle $\alpha = 0^\circ$ particles pass through the system undeviated like a collision-less gas. Near to $\alpha = 180^\circ$ in two dimensions deviation occurs because particles tend to move back and forth colliding repeatedly with their nearest neighbours. This violates the principle of molecular chaos used to derive the theoretical expression. The simulation results for η_{xy}^{kin} and η_{yx}^{kin} lie on the same curve, which confirms that the kinetic stress tensor is symmetric.

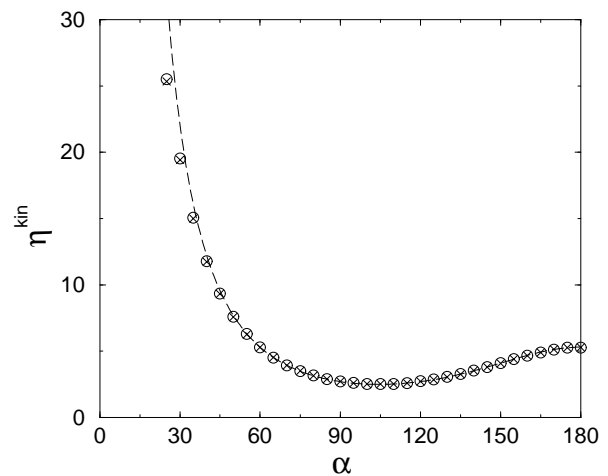
We obtained the collisional contribution to the shear viscosity in a similar manner by measuring the average momentum crossing a plane during the collision steps. Figure 3 compares the results of the simulations with the theoretical expressions (71) and (73). Again agreement is good. We verify clearly that the collisional shear stress tensor is not symmetric. This suggests that stochastic rotation dynamics should only be used in the regime of relatively high temperature, for which the kinetic contribution to the viscosity is dominant.

B. Thermal conductivity

We now aim, by setting up a temperature gradient and measuring the resulting energy flux, to directly measure the thermal conductivity and compare it to the theoret-



(a) Two dimensions

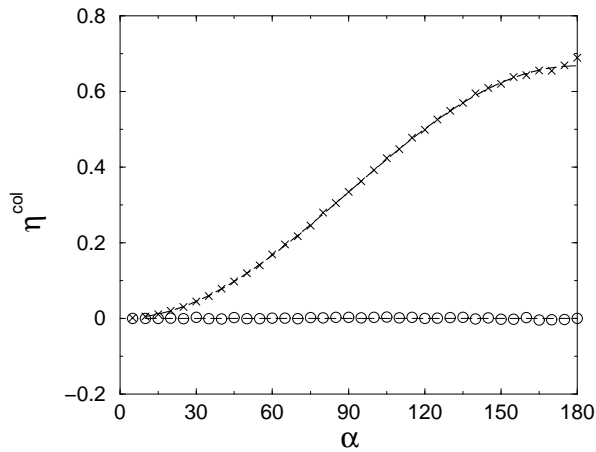


(b) Three dimensions

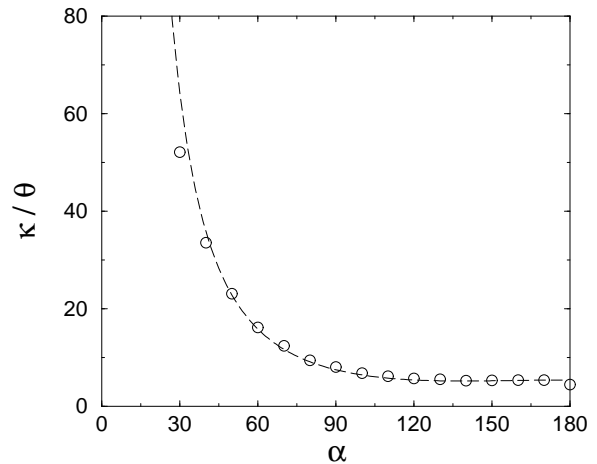
FIG. 2: Kinetic viscosity as a function of rotation angle α measured by considering a system under shear ($\times \eta_{xy}^{kin}$ simulation results for a plane parallel to the shear, $\circ \eta_{yx}^{kin}$ simulation results for a plane perpendicular to the shear, and - - - theory).

ical expression (64). A system of size $L_x = 100$ and $L_y = 50$ was used in two dimensions, and $L_x = 100$, $L_y = 5$ and $L_z = 5$ in three dimensions. Periodic boundary conditions were applied. A temperature gradient was imposed by thermostating the region from $x = 0$ to $x = 20$ at a temperature $\theta_1 = 0.5$, and thermostating the region from $x = 50$ to $x = 70$ at a higher temperature $\theta_2 = 1.5$. The pressure in the system was constant so consequently there were density gradients present.

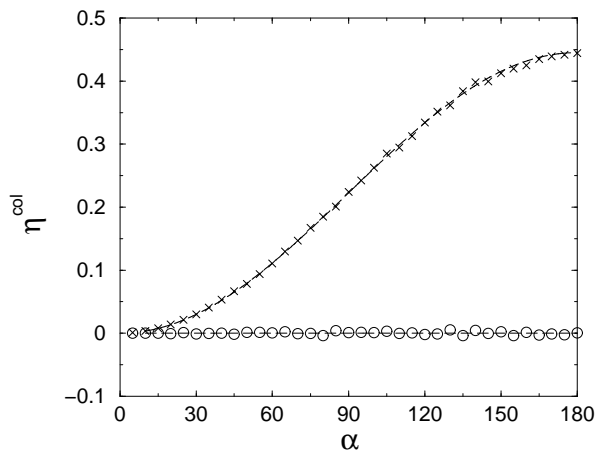
The energy flux across a plane and the temperature gradient were measured and the thermal conductivity



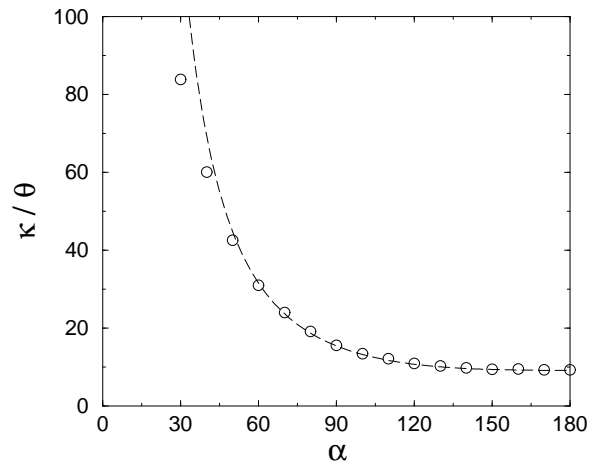
(a) Two dimensions



(a) Two dimensions



(b) Three dimensions



(b) Three dimensions

FIG. 3: Collisional viscosity as a function of rotation angle α measured by considering a system under shear ($\times \eta_{xy}^{col}$ simulation results for a plane parallel to the shear, $\circ \eta_{yx}^{col}$ simulation results for a plane perpendicular to the shear, and - - - theory).

calculated from their ratio. The measurement was made in the region where the average number density was $\gamma = 5$ and the statistical average was taken over 50000 time steps.

Figure 4 shows how the thermal conductivity changes as a function of rotation angle. The dashed lines represent the theoretical prediction (64). Good agreement is found. Deviation occurs within two regions. At small rotation angles particles interact only very weakly. Consequently their effective mean free path is very large. When this exceeds the size of the system, 30 in this case, deviation from the theory is inevitable. At rotation angles near to $\alpha = 180^\circ$ in two dimensions deviation results

FIG. 4: Thermal conductivity in units of $\theta = k_B T/m$ as a function of rotation angle α (\circ simulation results, and - - - theory).

from the breakdown of molecular chaos.

C. Choosing the average particle number per cell

We now discuss how quickly the simulation reaches a steady state and use this to motivate sensible choices of the rotation angle α and the average number of particles per cell γ .

As mentioned after equation (65) the viscosity relaxes to its steady state value on a time scale given by $\frac{\Delta t}{1-|w|}$. If we consider a system with no spatial gradients then

solving for the eigenvalues in equation (50) gives

$$\begin{pmatrix} M_{xxx} \\ M_{yyx} \end{pmatrix} = a_1 \lambda^t \begin{pmatrix} 1 \\ -1 \end{pmatrix} + a_2 \xi^t \begin{pmatrix} 3 \\ 1 \end{pmatrix},$$

$$\begin{pmatrix} M_{yyy} \\ M_{xxy} \end{pmatrix} = a_3 \lambda^t \begin{pmatrix} 1 \\ -1 \end{pmatrix} + a_4 \xi^t \begin{pmatrix} 3 \\ 1 \end{pmatrix}. \quad (74)$$

The amplitudes a_{1-4} reflect how far the system is from equilibrium initially. λ and ξ are functions of α and γ , and give a measure of how quickly the third order moments decay toward equilibrium. Hence, $\frac{\Delta t}{1-|\lambda|}$ and $\frac{\Delta t}{1-|\xi|}$ give the relaxation times for the thermal conductivity. Analytic expressions for λ and ξ were not possible, but they were evaluated numerically for the two dimensional algorithm.

We want all relaxation times to be as fast as possible and this motivates a suitable choice for γ . Figure 5(a) shows, as a function of α , which value of γ minimises the longest of the three timescales. Figure 5(b) shows the corresponding relaxation time in units of Δt . Because this relaxation time must be the quickest process in the system we suggest that typically α should be used within the range 50° to 130° and, correspondingly, the best choice for particle number per cell is roughly $\gamma = 3$.

IV. CONCLUSIONS

In this paper we have used a kinetic theory approach to derive analytically the continuum equations of the stochastic rotation dynamics model. Hence we were able to obtain analytic expressions for the viscosity and for the thermal conductivity. The derivation made the assumption of molecular chaos. We performed numerical simulations to test the theoretical predictions and found good agreement.

The viscous stress tensor was found to behave like an ideal gas except for a term derived from the collisions. This term was found not to be symmetric and therefore rather unphysical. However its contribution is small if the temperature is such that particles typically move one cell distance l in each time step.

By considering how the system relaxes towards the Maxwell Boltzmann distribution we find that in two dimensions, for quick relaxation of the viscosity and thermal conductivity to their theoretical expressions, a suitable choice for the average particle number per cell is around $\gamma = 3$. The rotation angle α used should be in the range 50° to 130° .

Stochastic rotation dynamics is finding application as a ‘hydrodynamic heat bath’ in the simulation of complex fluids. We hope that a better understanding of its transport properties will help interpret the results obtained.

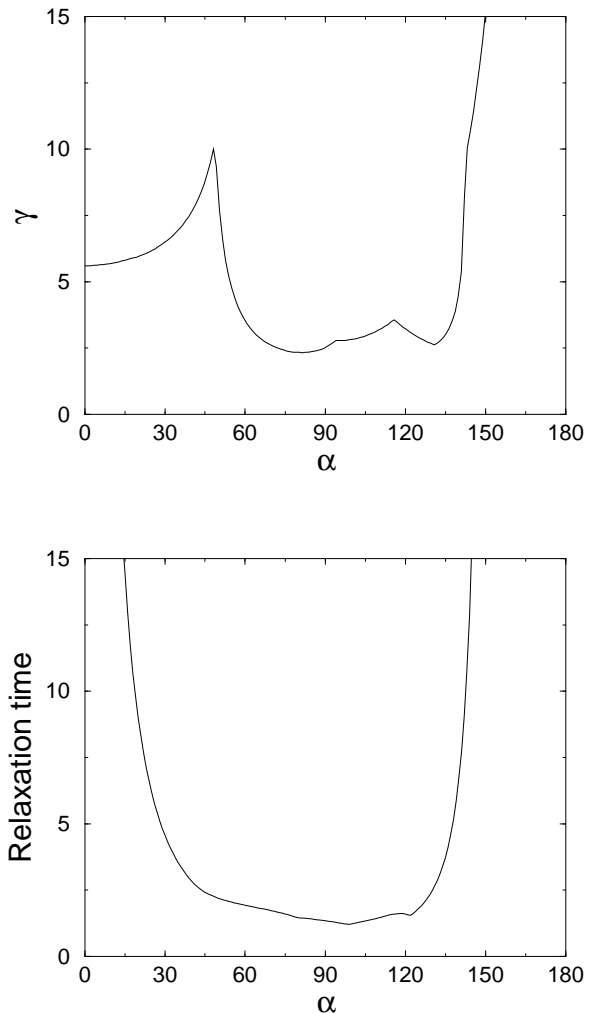


FIG. 5: (a) The average number of particles per cell γ which minimises the longest of the viscosity, $\frac{1}{1-|w|}$, and thermal conductivity, $\frac{1}{1-|\lambda|}$ and $\frac{1}{1-|\xi|}$, relaxation times, as a function of rotation angle α . (b) The corresponding relaxation time in units of Δt .

Acknowledgements

We thank D. Kroll, J. Ryder and N. Kikuchi for helpful discussions. We should particularly like to thank T. Ihle for his help in reconciling discrepancies between this paper and refs. [13, 14].

[1] Malevanets, A.; Kapral, R. *J. Chem. Phys.*, **1999**, 110, 8605.

[2] Kikuchi, N.; Gent, A.; Yeomans, J. M. *Eur. Phys. J. E*,

- 2002, 9, 63.
- [3] Malevanets, A.; Kapral, R. *J. Chem. Phys.*, **2000**, 112, 7260.
- [4] Falck, E.; Lahtinen, J. M.; Vattulainen, I.; Ala-Nissila, T. *Eur. Phys. J. E*, **2003**, 13, 267.
- [5] Lamura, A.; Gompper, G.; Ihle, T.; Kroll, D. M. *Europhys. Lett.*, **2001**, 56, 319.
- [6] Lamura, A.; Gompper, G.; Ihle, T.; Kroll, D. M. *Europhys. Lett.*, **2001**, 56, 768.
- [7] Lamura, A.; Gompper, G. *Eur. Phys. J. E*, **2002**, 9, 477.
- [8] Hashimoto, Y.; Chen, Y.; Ohashi, H. *Comput. Phys. Commun.*, **2000**, 129, 56.
- [9] Sakai, T.; Chen, Y.; Ohashi, H. *Phys. Rev. E*, **2002**, 65, 031503.
- [10] Tüzel, E.; Strauss, M.; Ihle, T.; Kapral, R. *Phys. Rev. E*, **2003**, 68, 036701.
- [11] Ihle, T.; Kroll, D. M. *Phys. Rev. E*, **2001**, 63, 020201.
- [12] Kikuchi, N.; Pooley, C. M.; Ryder, J. F.; Yeomans, J. M. *J. Chem. Phys.*, **2003**, 119, 6388.
- [13] Ihle, T.; Kroll, D. M. *Phys. Rev. E*, **2003**, 67, 066705.
- [14] Ihle, T.; Kroll, D. M. *Phys. Rev. E*, **2003**, 67, 066706.
- [15] Kubo, R. *Statistical Physics 2: Non-equilibrium Statistical Mechanics*; Springer Verlag, Germany, **1978**.
- [16] Landau, L. D.; Lifshitz, E. M. *Fluid mechanics, second edition*; Reed Educational and Professional Publishing Ltd, **1959**.
- [17] Lees, A. W.; Edwards, S. F. *J. Phys. C*, **1972**, 5, 1921.
- [18] Allen, M. P.; Tildesley, D. J. *Computer Simulation of Liquids*; Clarendon, Oxford, **1989**.